

Models of Chemical Evolution

FRANCESCA MATTEUCCI

University of Trieste, Astronomy Department, Via G.B. Tiepolo 11, 34100 Trieste, Italy

Abstract

The basic principles underlying galactic chemical evolution and the most important results of chemical evolution models are discussed. In particular, the chemical evolution of the Milky Way galaxy, for which we possess the majority of observational constraints, is described. Then, it is shown how different star formation histories influence the chemical evolution of galaxies of different morphological type. Finally, the role of abundances and abundance ratios as cosmic clocks is emphasized and a comparison between model predictions and abundance patterns in high redshift objects is used to infer the nature and the age of these systems.

1.1 Introduction

In order to build a chemical evolution model one needs to specify some basic parameters such as the boundary conditions, namely whether the system is closed or open and whether the gas is primordial or already chemically enriched. Then the stellar birthrate function, which is generally expressed as the product of two independent functions, the star formation rate (SFR) and the initial mass function (IMF), namely:

$$B(m,t) = \psi(t)\varphi(m) \tag{1.1}$$

where the SFR is assumed to be only a function of time and the IMF only a function of the stellar mass. The stellar evolution and nucleosynthesis are also necessary ingredients for modelling chemical evolution and in particular we need to specify the stellar yields ($p_i(m)$).

Then, one can include in the chemical evolution model some supplementary ingredients such as the the infall of extragalactic material, radial flows and galactic winds, which can play a more or less important role depending on the galactic system under study. In particular, gas infall and radial flows can be important in describing the chemical evolution of spiral disks, whereas galactic outflows are probably important in elliptical galaxies where the SFR was very high in the past and there is no cold gas at the present time, as well as in dwarf galaxies which possess a smaller potential well. In fact, galactic outflows, which eventually can transform into galactic winds, are determined by two main processes; the supernova feedback, namely how much energy is transferred from SNe into the interstellar medium (ISM), and the galactic potential well.

F. Matteucci

In this paper, I will recall the most popular approximations used to describe both the basic and the supplementary ingredients involved in galactic chemical evolution. Then I will describe detailed numerical models which can follow the evolution in space and time of the abundances of the most abundant chemical species. I will show some applications of such models to the Milky Way galaxy and then to galaxies of different morphological type, focussing on the fact that abundances and abundance ratios are very useful tools to infer the history of star formation in galaxies, to impose constraints on the stellar nucleosynthesis and to derive information on the nature and the age of high redshift objects.

1.2 The star formation rate

The SFR is one of the most important drivers of galactic chemical evolution: it describes the rate at which the gas is turned into stars in galaxies. Since the physics of the star formation process is still not well known, several parametrizations are used to describe the SFR. A common aspect to the different formulations of the SFR is that they include a dependence upon the gas density. Here I recall the most commonly used parametrizations for the SFR adopted so far in the literature.

An exponentially decreasing SFR provides an easy to handle formula:

$$SFR = \nu e^{-t/\tau_*} \quad (1.2)$$

with $\tau_* = 5 - 15$ Gyr in order to obtain a good fit to the properties of the solar neighbourhood (Tosi, 1988) and $\nu = 1 - 2 \text{Gyr}^{-1}$, being the so-called efficiency of star formation which is expressed as the inverse of the timescale of star formation.

However, the most famous formulation and most widely adopted for the SFR is the Schmidt (1955) law:

$$SFR = \nu \sigma_{gas}^k \quad (1.3)$$

which assumes that the SFR is proportional to some power of the volume or surface gas density. The exponent suggested by Schmidt was $k = 2$ but Kennicutt (1998) suggested that the best fit to the observational data on spiral disks and starburst galaxies is obtained with an exponent $k = 1.4 \pm 0.15$.

A more complex formulation, including a dependence also from the total surface mass density, which is induced by the SN feedback, was suggested by the observations of Dopita & Ryder (1994) who proposed the following formulation:

$$SFR = \nu \sigma_{tot}^{k_1} \sigma_{gas}^{k_2} \quad (1.4)$$

with $1.5 < k_1 + k_2 < 2.5$.

Kennicutt suggested also an alternative law to the Schmidt-like one discussed above, in particular a law containing the angular rotation speed of gas, Ω_{gas} :

$$SFR = 0.017 \Omega_{gas} \sigma_{gas} \propto R^{-1} \sigma_{gas} \quad (1.5)$$

A similar law for the SFR taking into account star formation induced by spiral density waves was proposed by Wyse & Silk (1989) and it can be expressed as (Prantzos 2002):

$$SFR = \nu V(R) R^{-1} \sigma_{gas}^{1.5} \quad (1.6)$$

F. Matteucci

where $V(R)$ is the rotational velocity in the disk and R is the galactocentric distance. It is worth noting that the SFRs expressed by eqs. (1.4), (1.5) and (1.6) contain a stronger dependence on the radial properties of the disk than the simple Schmidt law, and this characteristic is required to best fit the disk properties (see next sections).

1.3 The IMF

The most common parametrization for the IMF is that proposed by Salpeter (1955), which assumes a one-slope power law with $x = 1.35$, in particular:

$$\varphi(M) = cM^{-(1+x)} \quad (1.7)$$

is the number of stars with masses in the interval $M, M+dM$, and c is a normalization constant.

The IMF is generally normalized as:

$$\int_0^\infty M\varphi(M)dM = 1 \quad (1.8)$$

More recently, multi-slope (x_1, x_2, \dots) expressions of the IMF have been adopted since they are better describing the luminosity function of the main sequence stars in the solar vicinity (Scalo 1986, 1998; Kroupa et al. 1993). Generally, the IMF is assumed to be constant in space and time, with some exceptions such as the one suggested by Larson (1998), which adopts a variable slope:

$$x = 1.35(1 + m/m_1)^{-1} \quad (1.9)$$

where m_1 is variable with time and associated to the Jeans mass. The effects of a variable IMF on the galactic disk properties have been studied by Chiappini et al. (2000), who concluded that only a very ‘‘ad hoc’’ variation of the IMF can reproduce the majority of observational constraints, thus favoring chemical evolution models with IMF constant in space and time.

1.4 Infall and outflow

Depending on the galactic system, the infall rate can be assumed to be constant in space and time, or more realistically the infall rate can be variable in space and time:

$$IR = A(R)e^{-t/\tau(R)} \quad (1.10)$$

with $\tau(R)$ constant or varying along the disk. The parameter $A(R)$ is derived by fitting the present time total surface mass density in the disk of the Galaxy, $\sigma_{tot}(t_G)$. Otherwise, for the formation of the Galaxy one can assume two independent episodes of infall during which the halo and perhaps part of the thick-disk formed first and then the thin-disk, respectively:

$$IR = A(R)e^{-t/\tau_H(R)} + B(R)e^{-(t-t_{max})/\tau_D(R)} \quad (1.11)$$

as in the two-infall model of Chiappini et al. (1997). Here τ_H is the timescale for the formation of the halo/thick disk and $\tau_D(R)$ is the timescale for the formation of the thin-disk. This latter is assumed to increase linearly with galactocentric distance (Matteucci & François 1989; Chiappini et al. 1997; Boissier & Prantzos 1999). For the rate of gas outflow or galactic wind there are no specific prescriptions but generally one simply assumes that the

F. Matteucci

wind rate is proportional to the star formation rate through a suitable parameter (Hartwick, 1976; Matteucci & Chiosi, 1983):

$$W = -\lambda SFR \quad (1.12)$$

with λ being a free parameter.

1.5 Stellar Yields

The stellar yields are fundamental ingredients in galactic chemical evolution. In order to introduce the stellar yields we recall some useful concepts and define the *yield per stellar generation*.

Under the assumption of Instantaneous Recycling Approximation (I.R.A.) we define the yield per stellar generation of a given element i as (Tinsley, 1980):

$$y_i = \frac{1}{1-R} \int_1^\infty m p_{im} \varphi(m) dm \quad (1.13)$$

where p_{im} is the stellar yield of the element i , namely the newly formed and ejected mass fraction of the element i by a star of initial mass m . It is worth noting that the expression (1.13) is an oversimplification and it does not have much meaning when considering chemical elements formed on long timescales. The quantity R is the returned fraction:

$$R = \int_1^\infty (m - M_{rem}) \varphi(m) dm \quad (1.14)$$

where M_{rem} is the remnant mass of a star of mass m . In the past ten years a large number of calculations of the stellar yields, p_{im} , has become available for stars of all masses and metallicities. However, uncertainties in stellar yields are still present especially in the yields of Fe-peak elements. This is due to uncertainties in the nuclear reaction rates, treatment of convection, mass cut, explosion energies, neutron fluxes and possible fall-back of matter on the proto-neutron star. Moreover, the ^{14}N nucleosynthesis and its primary and/or secondary nature are still under debate. The most recent calculations are summarized below:

- Low and Intermediate mass stars ($0.8 \leq M/M_\odot \leq 8.0$) (Marigo et al. 1996; van den Hoek & Groenewegen 1997; Meynet & Maeder, 2002; Ventura et al. 2002; Siess et al. 2002). These stars produce ^4He , C, N and some s-process ($A > 90$) elements.
- Massive stars ($M \geq 10M_\odot$) (Woosley & Weaver 1995; Langer & Henkel 1995; Thielemann et al. 1996; Nomoto et al. 1997; Rauscher et al. 2002; Limongi & Chieffi 2003). These stars produce mainly α -elements (O, Ne, Mg, Si, S, Ca), some Fe-peak elements, s-process elements ($A < 90$) and r-process elements.
- Type Ia SNe (Nomoto et al. 1997; Iwamoto et al. 1999) produce mainly Fe-peak elements.
- Very massive objects ($M > 100M_\odot$), if they exist, should produce mostly oxygen (Portinari et al. 1998; Umeda & Nomoto 2001; Nakamura et al. 2001).

In Figures 1.1 and 1.2 we show a comparison between the yields, produced in massive stars, of two α -elements (O and Mg) and Fe, respectively, as predicted by different authors. As is evident from Fig. 1.1 the O yields from different sources seem to be in good agreement with one another. The yields of Mg, especially the most recent ones seem to be also in good agreement with each others, whereas for the yields of Fe (Figure 1.2) there is not yet an agreement among different authors. Observational estimates of Fe produced in type II SNe (Elmhamdi et al. 2003) can help in constraining the Fe yields in massive stars.

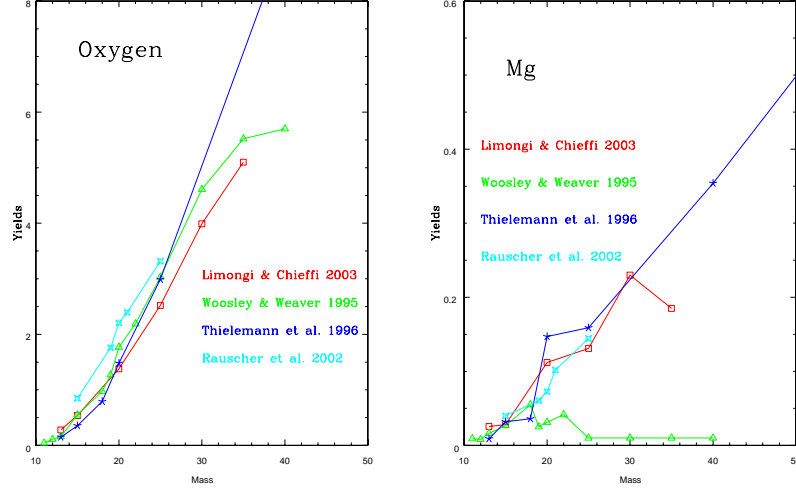


Fig. 1.1. Comparison between different yields of oxygen and Mg from SNII: open triangles, Woosley & Weaver (1995); open squares, Limongi & Chieffi (2003); stars, Thielemann et al. (1996); four-point stars, Rauscher et al. (2002).

1.6 Analytical models of chemical evolution

The simplest model of galactic chemical evolution is the so-called *Simple Model* for the evolution of the solar neighbourhood. We define the solar neighbourhood or solar vicinity as a cylinder centered in the Sun with 1 kpc radius.

The basic assumptions of the Simple Model can be summarized as follows:

- the system is one-zone and closed, no inflows or outflows
- the initial gas is primordial (no metals)
- the instantaneous recycling approximation holds (I.R.A.)
- $\varphi(m)$ is constant in time and space
- the gas is well mixed at any time (I.M.A.)

Let X_i be the abundance of an element i and $\beta = \frac{M_{\text{gas}}}{M_{\text{tot}}}$ the ratio between the mass of gas and the total mass of the system. If $X_i \ll 1$, which is generally true for metals, then we can write:

$$X_i = y_i \ln\left(\frac{1}{\beta}\right) \quad (1.15)$$

which is the well known solution for the Simple Model, where y_i is the yield per stellar generation as defined in eq. (1.13). In particular, the yield appearing in eq. (1.15) is usually referred to as the *effective yield*. If X_i is not much lower than 1, as is the case for X_{He} (Maeder 1992), a more precise expression for the solution of the Simple Model is given by:

$$X_i = 1 - \beta^{y_i} \quad (1.16)$$

It is worth noting that generally, in I.R.A., we can assume:

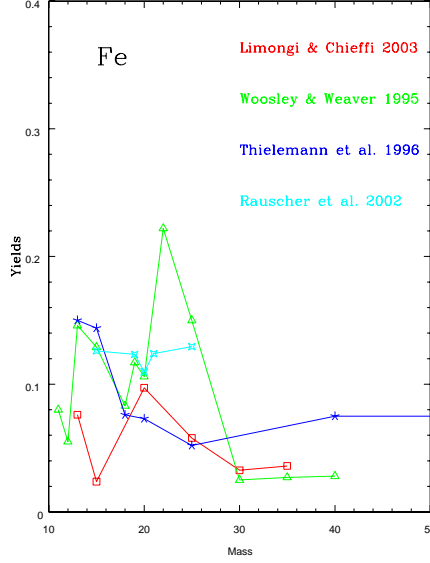


Fig. 1.2. Comparison between different yields of iron from SNI: open triangles, Woosley & Weaver (1995); open squares Limongi & Chieffi (2003); stars Thielemann et al. (1996); four-point stars Rauscher et al. (2002).

$$\frac{X_i}{X_j} = \frac{y_i}{y_j} \quad (1.17)$$

namely that the abundance ratios are equivalent to the yield ratios, and this holds also in analytical models with infall and/or outflow. Clearly, eq. (1.17) can be used safely only for elements produced on short timescales, such as α -elements, but it fails if applied to elements produced on long timescales such as Fe and N. These days the Simple Model is rarely used in describing the chemical evolution of the Milky Way since it does not reproduce the G-dwarf metallicity distribution (the G-dwarf problem) as well as the elements produced on long timescales such as Fe (Matteucci, 2001).

1.7 Numerical models of chemical evolution

In the last years a great number of models relaxing I.R.A. and the closed box assumption but retaining the constancy of the IMF and the I.M.A., have appeared in the literature. As an example of the basic equations adopted in such models I show the formulation of Matteucci & Greggio (1986), which is based on the original formulations of Talbot & Arnett (1971) and Chiosi (1980).

Let G_i be the mass fraction of gas in the form of an element i ($\sigma_i/\sigma_{tot}(t_G)$), we can write:

$$\begin{aligned} \dot{G}_i(t) = & -\psi(t)X_i(t) + \int_{M_L}^{M_{Bm}} \psi(t-\tau_m)Q_{mi}X_i(t-\tau_m)\phi(m)dm + \\ & + A \int_{M_{Bm}}^{M_{BM}} \phi(m) \cdot \left[\int_{\mu_{min}}^{0.5} f(\mu)\psi(t-\tau_{m2})Q_{mi}X_i(t-\tau_{m2})d\mu \right] dm + \end{aligned}$$

F. Matteucci

$$\begin{aligned}
& + (1-A) \int_{M_{BM}}^{M_{BM}} \psi(t-\tau_m) Q_{mi} X_i(t-\tau_m) \phi(m) dm + \\
& + \int_{M_{BM}}^{M_U} \psi(t-\tau_m) Q_{mi} X_i(t-\tau_m) \phi(m) dm + X_{A_i} IR(t) - X_i W(t)
\end{aligned} \tag{1.18}$$

where A is a constant parameter chosen in order to fit the present time SN Ia rate and it lies in the range $A=0.05-0.09$. The SNIa rate should be based on the existing theories on SN Ia progenitors which I will summarize in the next section. In the equations above the type Ia SNe are assumed to originate from C-O white dwarfs (WD) in binary systems and $f(\mu)$ represents the distribution of mass ratios in such binary systems ($\mu = \frac{M_2}{(M_1+M_2)}$) (see Matteucci & Recchi, 2001 for more details). The star formation rate $\psi(t)$ and all the rates in this equations are expressed as functions of the fraction of gas ($G = \frac{\sigma_{gas}}{\sigma_{tot}(t_G)}$). The quantities $IR(t)$ and $W(t)$ represent the rate of gas accretion and the rate of galactic outflow (wind), respectively, and X_{A_i} are the abundances of the accreting material, which are usually assumed to be primordial (no metals). Generally, in describing the solar neighbourhood and the Galactic disk one assumes $W(t) = 0$, whereas the infall of mostly primordial material is most likely to be responsible for the formation of the disk.

1.7.1 Type Ia SN progenitors

The single degenerate scenario is the classical scenario originally proposed by Whelan and Iben (1973), namely C-deflagration in a C-O WD reaching the Chandrasekhar mass limit, $M_{Ch} \sim 1.44M_{\odot}$, after accreting material from a red giant companion. The progenitors of C-O WDs lie in the range $0.8-8.0M_{\odot}$, therefore, the most massive binary system of two C-O WDs is the $8M_{\odot} + 8M_{\odot}$ one. The clock of the system in this scenario is provided by the lifetime of the secondary star (i.e. the less massive one in the binary system). This implies that the minimum timescale for the appearance of the first type Ia SNe is the lifetime of the most massive secondary star. In this case the time is $t_{SNIa_{min}} = 0.03$ Gyr (Greggio and Renzini 1983a; Matteucci & Greggio, 1986; Matteucci & Recchi, 2001).

The double degenerate scenario consists in the merging of two C-O WDs, due to loss of angular momentum occurring as a consequence of gravitational wave radiation, which then explode by C-deflagration when the M_{Ch} is reached (Iben and Tutukov 1984). In this case the minimum timescale for the appearance of type Ia SNe is the lifetime of the most massive secondary star plus the gravitational time delay which depends on the original separation of the two WDs and which is computed according to Landau & Lifschitz (1962), namely $t_{SNIa_{min}} = 0.03 + \Delta t_{grav} = 0.03 + 0.15$ Gyr (Tornambè & Matteucci, 1986). We recall that the gravitational time delay can be as long as several Hubble times.

The model by Hachisu et al. (1999) is based on the classical scenario of Whelan & Iben (1973) but with a metallicity effect implying that no type Ia systems can form for $[Fe/H] < -1.0$ dex in the ISM. This implies a much longer time delay for the first type Ia SNe to occur, also because the maximum masses of the secondary stars in the binary systems are assumed to be $\leq 2.6M_{\odot}$. Therefore, in this case $t_{SNIa_{min}} = 0.33$ Gyr + metallicity delay due to the chemical evolution of the considered system. In this scenario, type Ia SNe are not associated with young stellar populations contrary to what is suggested by a recent search for SNe Ia in starburst galaxies (see Mannucci et al. 2003), which seem to favor the scenario where the progenitors of type Ia SNe can be as high as $8M_{\odot}$.

Clearly, $t_{SNIa_{min}}$ is a very important parameter for computing galactic chemical evolution

F. Matteucci

since the abundance patterns will depend strongly on this timescale, although the most important timescale is the one for which the type Ia SNe have an impact on the abundances of the ISM. In successful models of galactic chemical evolution of the solar vicinity this timescale is 1.0-1.5 Gyr in the framework of the single degenerate model (Matteucci & Greggio, 1986). In the other two scenarios this time is longer, especially in the one including the metallicity effect and it varies with different histories of star formation (see Matteucci & Recchi 2001 and sect. 1.13).

1.8 Different approaches to the formation and evolution of the Galaxy

In the past years several approaches to the calculation of the chemical evolution of the Galaxy were proposed, they are:

- i) **the serial formation**, where the halo, thick and thin disk form in a sequence as a continuous process (e.g. Matteucci & François 1989).
- ii) **The parallel formation** where the various Galactic components start forming at the same time and from the same gas but evolve at different rates. This approach predicts overlapping of stars belonging to the different components (e.g. Pardi, Ferrini & Matteucci 1995) but it does not provide a good fit to the G-dwarf metallicity distribution and the halo star metallicity distribution simultaneously, as discussed in Matteucci (2001).
- iii) **The two-infall approach** where the halo and disk form out of two separate infall episodes from extragalactic gas. Also in this case we predict an overlap in metallicity between the different galactic components (e.g. Chiappini et al. 1997; Chang et al. 1999). A threshold density ($\sigma_{th} = 7M_{\odot}pc^{-2}$) in the star formation process is also included in the model of Chiappini et al. (1997).
- iv) **The stochastic approach** where the assumption is made that in the early halo phases, mixing was not efficient and pollution from single SNe would dominate the galactic enrichment (Tsujiimoto et al. 1999; Argast et al. 2000; Oey 2000). In this case a large spread in the abundances and abundance ratios at low metallicities is predicted. This predicted spread, however, is much larger than observed, especially for α -elements.

1.9 Observational Constraints

A good model of chemical evolution should be able to reproduce a minimum number of observational constraints and the number of observational constraints should be larger than the number of free parameters which are: τ_H , τ_D , k_1 , k_2 , ν , the IMF slope(s) and the parameter describing the wind, if adopted.

The main observational constraints in the solar vicinity that a good model should reproduce (see Chiappini et al. 2001) are:

- The present time surface gas density: $\Sigma_G = 13 \pm 3M_{\odot}pc^{-2}$
- The present time surface star density $\Sigma_* = 48 \pm 9M_{\odot}pc^{-2}$
- The present time total surface mass density: $\Sigma_{tot} = 51 \pm 6M_{\odot}pc^{-2}$
- The present time SFR: $\psi_o = 2 - 5M_{\odot}pc^{-2}Gyr^{-1}$
- The present time infall rate: $0.3 - 1.5M_{\odot}pc^{-2}Gyr^{-1}$
- The present day mass function (PDMF)
- The solar abundances, namely the chemical abundances of the ISM at the time of birth of the solar system 4.5 Gyr ago and the present time abundances
- The observed $[X/Fe]$ vs. $[Fe/H]$ relations
- The G-dwarf metallicity distribution

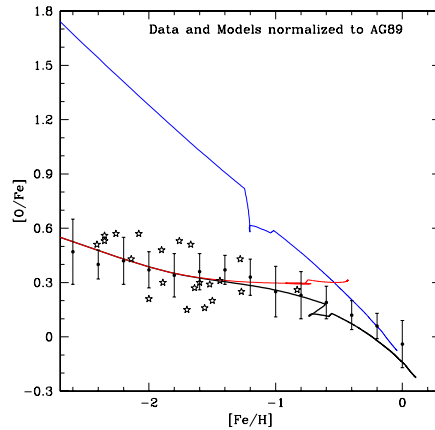


Fig. 1.3. Time-delay model. The models and the data are normalized to the solar abundances of Anders & Grevesse 1989. The thick curve represents the predictions of the standard time-delay model where type Ia SN produce 70% of Fe and type II SNe the remaining 30%. The figure is from Matteucci & Chiappini, 2003 in preparation)

- The age-metallicity relation

And finally, a good model of chemical evolution of the Milky Way should reproduce the distributions of abundances, gas and star formation rate along the disk as well as the average SNI_{II} and Ia rates along the disk (SNI_{II}= 1.2 ± 0.8 100yr⁻¹ and SNI_a= 0.3 ± 0.2 100yr⁻¹)

1.10 Time-delay model interpretation

The difference in the timescales for the occurrence of SNI_{II} and Ia produces a time-delay in the Fe production relative to the α -elements (Tinsley 1979; Greggio & Renzini 1983b; Matteucci 1986). On this basis we can interpret all the observed abundance ratios plotted as functions of metallicity. In particular, this interpretation is known as time-delay model and can be easily illustrated by Figure 1.3, where we show the predictions of the two-infall model for the chemical evolution of the solar vicinity concerning the [O/Fe] vs. [Fe/H] relation. We show the standard case in which both the contributions to Fe enrichment from type II and Ia are taken into account as well as the cases where only one type of SN at the time is assumed to contribute to Fe enrichment. Both data and models are normalized to the solar abundances (Anders & Grevesse 1989). From the Figure 1.3 is evident that only type Ia SNe as Fe producers would predict a continuous decrease of the [O/Fe] ratio from low to high metallicities (upper curve), whereas only type II SNe would create a roughly constant [O/Fe] ratio. Therefore, only a model including both contributions in the percentages of 30% (SNI_{II}) and 70%(SNI_a) can reproduce the data.

The time-delay model, with the assumption of an IMF constant in time, can explain the different abundance patterns in the halo, disk and bulge (see Matteucci, 2001).

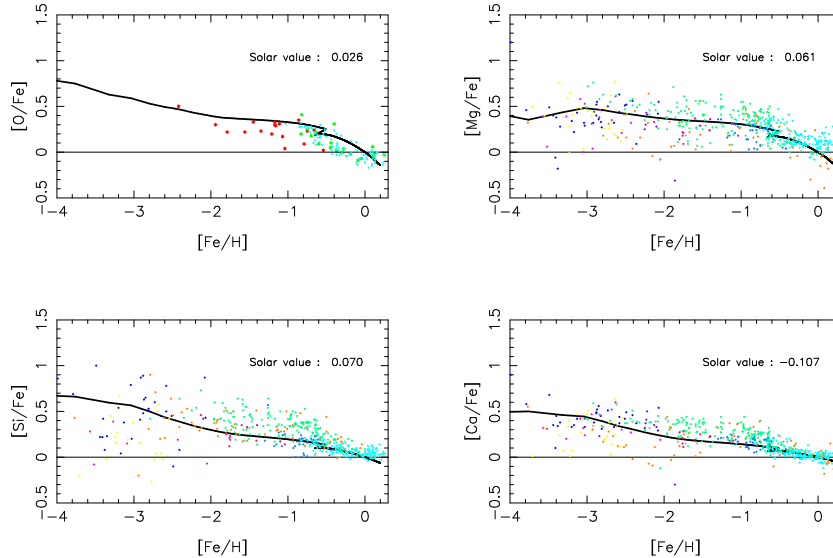


Fig. 1.4. Predicted and observed $[\alpha/\text{Fe}]$ vs. $[\text{Fe}/\text{H}]$ in the solar neighbourhood. The model is from Chiappini et al. (1997) whereas the data are from François et al. (2003). The models are normalized to the predicted solar abundances. The predicted abundance ratios at the time of the Sun formation are shown in each panel and indicate a good fit.

1.11 Common Conclusions from Galaxy Models

Most of the more recent chemical evolution models agree on several important issues which are: i) the G-dwarf metallicity distribution can be reproduced only by assuming that the formation of the local disk occurred by infall of extragalactic gas on a long timescale, of the order of $\tau_d \sim 6-8$ Gyr (Chiappini et al. 1997; Boissier and Prantzos 1999; Chang et al. 1999; Chiappini et al. 2001; Alibès et al. 2001)

ii) The relative abundance ratios $[X_i/\text{Fe}]$ vs. $[\text{Fe}/\text{H}]$, interpreted as being due to time-delay between type Ia and II SNe allow one to reproduce the observed relations (see Figure 1.4) and to infer the timescale for the halo-thick disk formation (corresponding to $[\text{Fe}/\text{H}]=-1.0$ dex) which should be of the order of $\tau_h \sim 1.5$ Gyr (Matteucci and Greggio 1986; Matteucci and François, 1989; Chiappini et al. 1997). On the other hand, the external halo formed more slowly, perhaps on timescales of the order of 3-4 Gyr (see Matteucci & François 1992). In Figure 1.4 we show the predictions of the model developed by Chiappini et al. (1997), by adopting the yields of Woosley & Weaver (1995) for type II SNe, with the exception of the Mg yields which have been artificially increased by a factor of 5 to obtain a good agreement with the solar abundance of Mg, and those of Nomoto et al. (1997) for type Ia SNe (their case W7). The Mg yield in type Ia SNe had also to be increased in order to fit the solar abundances (François et al. 2003, in preparation). The problem of Mg underproduction in nucleosynthesis models is well known and it was pointed out by Thomas et al. (1998). Figure 1.4 shows clearly that the agreement between the model predictions and data for α -elements is quite good and support the time-delay model.

iii) To fit abundance gradients, SFR and gas distributions along the disk, the disk should

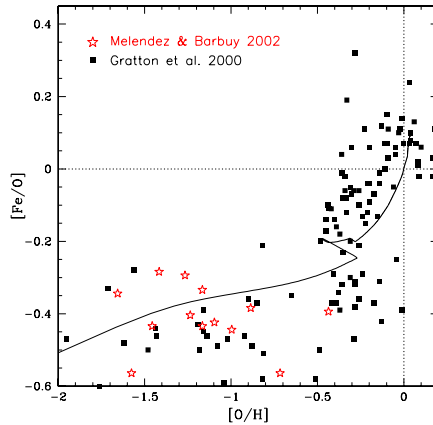


Fig. 1.5. Gap in the SFR. The model predictions for $[\text{Fe}/\text{O}]$ vs. $[\text{Fe}/\text{H}]$ are obtained by means of the two-infall model (see text). As one can see a gap seems to be evident at $[\text{O}/\text{H}] \sim -0.3$ dex.

have formed inside-out (variable τ_D) and the SFR should be a strongly varying function of the galactocentric distance as in eqs. (1.4), (1.5) and (1.6) (Matteucci & François 1989; Chiappini et al, 1997,2001; Portinari & Chiosi, 1999, Goswami & Prantzos 2000; Alibés et al. 2001).

1.12 Specific Conclusions from Galaxy Models

The assumed threshold in the SFR (Chiappini et al. 1997) produces naturally a gap in the star formation process between the end of the halo-thick disk phase and the beginning of the thin disk phase. Such a gap lasts for ~ 1 Gyr and it seems to be indicated by the observations (Gratton et al. 2000). In particular, in Figure 1.5 we show the observed and predicted $[\text{Fe}/\text{O}]$ vs. $[\text{O}/\text{H}]$, where it appears that at around $[\text{O}/\text{H}] = -0.3$ dex there is a lack of stars and then the $[\text{Fe}/\text{O}]$ ratio rises sharply. This is a clear indication, on the basis of the time-delay model, that there has been a period when only Fe was produced, in other words a halt in the SFR. This gap seems to be observed also in the $[\text{Fe}/\text{Mg}]$ vs. $[\text{Mg}/\text{H}]$ (Furhmann, 1998). However, more data are necessary before drawing firm conclusions on this important point (see also Chiappini & Matteucci, this conference).

No agreement on the behaviour of gradients in time exists among different authors. In particular, some authors e.g. (Boissier and Prantzos 1998; Portinari & Chiosi, 1999, Alibès et al. 2001) find a flattening of abundance gradients with time whereas others (Matteucci & François, 1989; Chiappini et al. 2001) predict a steepening of the abundance gradients, in agreement with results from chemo-dynamical models (Samland et al. 1997). The difference between the two different approaches assumed by the various authors could perhaps reside in the different star formation and/or infall laws adopted for the Galactic disk (see Tosi, 2000 for a discussion of this point). Data from planetary nebulae (PNe) of different ages can help in solving this problem; recently Maciel et al. (2002) suggested a flattening of the gradients with time. In any case, all the models predict a very small evolution in the last 5 Gyr.

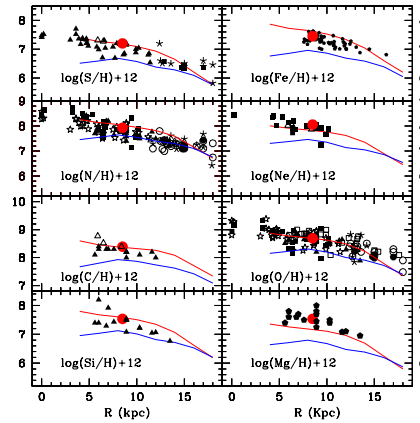


Fig. 1.6. Abundance gradients along the Galactic disk and their evolution in time, as predicted by the model of Chiappini et al. (2001). The lower curve of each panel represents the model prediction after 2 Gyr from the beginning of star formation in the thin-disk. The upper curve represent the predicted gradient at the present time.

1.13 Star formation rate in galaxies

It is very important to understand that different histories of star formation determine the abundance patterns in galaxies. In particular, the $[X_i/\text{Fe}]$ vs. $[\text{Fe}/\text{H}]$ relations are strongly influenced by the SFR which influences the temporal growth of the Fe abundance.

In other words, the time-delay model coupled with different SF histories implies different timescales for the bulk of Fe production from type Ia SNe, thus producing different $[\alpha/\text{Fe}]$ vs. $[\text{Fe}/\text{H}]$ relations in different objects. The typical timescale for type Ia SN enrichment can be defined as the time when the SN Ia rate reaches the maximum $t_{\text{SN Ia}}$ (Matteucci & Recchi 2001). This timescale depends upon the progenitor lifetimes, the IMF and the SFR. For an elliptical galaxy or a bulge of a spiral with high SFR the maximum in the type Ia SN rate is reached at $t_{\text{SN Ia}} = 0.3 - 0.5$ Gyr, whereas for a spiral like the Milky Way a first maximum in the SN Ia rate is reached at $t_{\text{SN Ia}} = 1.5$ Gyr and a second maximum, if one uses the two-infall model, at $t_{\text{SN Ia}} = 4 - 5$ Gyr. Therefore, for the Milky Way 1-1.5 Gyr is the time at which SNe Ia are no more negligible in the process of chemical enrichment and it corresponds to the change in slope observed in the $[\alpha/\text{Fe}]$ vs. $[\text{Fe}/\text{H}]$ relations (Figure 1.4) and to the end of the halo phase. For an irregular galaxy, where the SFR is assumed to proceed more slowly than in the solar vicinity the timescale for SN Ia enrichment is $t_{\text{SN Ia}} = 7 - 8$ Gyr. Therefore, it is worth repeating that the $t_{\text{SN Ia}}$ is different in different galaxies, since often in the literature it is adopted a universal timescale of 1 Gyr! On the basis of that we expect that objects where the SFR proceeds very fast such as in the spheroids (bulges and ellipticals), the $[\alpha/\text{Fe}]$ ratio stays flat for a larger metallicity interval than in systems with slower star formation such as the Milky Way, and that eventually the $[\alpha/\text{Fe}]$ ratios in irregulars, where the star formation rate has been less efficient than in spiral, decreases almost continuously, as shown in Figure 1.7. The models shown in Figure 1.7 contain the same nucleosynthesis prescriptions and differ for the star formation history.

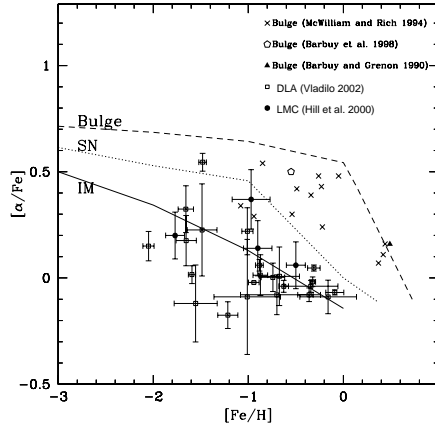


Fig. 1.7. The predicted $[\alpha/\text{Fe}]$ vs. $[\text{Fe}/\text{H}]$ in different objects. Data for the Galactic bulge, the LMC and Damped Lyman- α systems are shown for comparison.

1.14 High-redshift objects

In Figure 1.7 we show also some observational data relative to the Galactic bulge, the LMC and some Damped Lyman- α systems (DLA). As one can see, our predictions seem to reproduce the data for the Galactic bulge and for LMC and also suggest that DLAs could be the progenitors of the present day irregular galaxies, since most of DLAs, once their abundances are corrected for the effect of dust, show low $[\alpha/\text{Fe}]$ ratios at low metallicities (Vladilo, 2002; Calura et al. 2003). On the other hand, Lyman-break galaxies such as cB58 (Pettini et al. 2002) show an abundance pattern compatible with a young spheroid, either a galactic bulge or a small elliptical, suffering a galactic outflow, as recently shown by Matteucci & Pipino (2002). Therefore, the $[X_i/\text{Fe}]$ vs. $[\text{Fe}/\text{H}]$ diagram represents a very useful tool to infer the nature of high redshift objects of which we know just the abundances and abundance ratios.

References

- Alibés, A., Labay, J., Canal, R. 2001, A&A, 370, 1103
 Anders, E., Grevesse, N. 1989, Geochim. Cosmochim. Acta, 53, 197
 Argast, D., Samland, M., Gerhard, O.E., Thielemann, F.-K. 2000, A&A, 356, 873
 Barbuy, B., Grenon, M. 1990, in ESO/CTIO Workshop on Bulges of Galaxies, ESO Publ. p.83
 Barbuy, B., Ortolani, S., Bica, E. 1998, A&AS, 132, 333
 Boissier, S., Prantzos, N. 1999, MNRAS, 307, 857
 Calura, F., Matteucci, F., Vladilo, G. 2003, MNRAS, 340, 59
 Chang, R.X., Hou, J.L., Shu, C.G., Fu, C.Q. 1999, A&A, 350, 38
 Chiappini, C., Matteucci, F., Gratton, R. 1997, ApJ, 477, 765
 Chiappini, C., Matteucci, F., Padoan, P. 2000, ApJ, 528, 711
 Chiappini, C., Matteucci, F., Romano, D. 2001, ApJ, 554, 1044
 Chiosi, C. 1980, A&A, 83, 206
 Dopita, M.A., Ryder, S.D. 1994, ApJ, 430, 163
 Elmhamdi, A., Chugai, N.N., Danziger, I.J. 2003, A&A, in press
 Fuhrmann, K., 1998, A&A, 338, 161

F. Matteucci

- Goswami, A., Prantzos, N. 2000, *A&A*, 359, 191
Gratton, R.G., Carretta, E., Matteucci, F., Sneden, C. 2000, *A&A*, 358, 671
Greggio, L., Renzini, A. 1983a, *A&A*, 118, 217
Greggio, L., Renzini, A. 1983b in "The First Stellar Generations", *Mem. Soc. Astron. It.*, Vol. 54, p.311
Kennicutt, R.C. Jr. 1998, *ApJ*, 498, 541
Kroupa, P., Tout, C.A., Gilmore, G. 1993, *MNRAS*, 262, 545
Hachisu, I, Kato, M., Nomoto, K. 1999, *ApJ*, 522, 487
Hartwick, F. 1976, *ApJ*, 209,418
Hill, V., François, P., et al. 2000, *A&A*, 364, L19
Iben, I.Jr., Tutukov, A.V. 1984, *ApJS*54, 335
Iwamoto, N., Brachwitz, F. et al. 1999, *ApJS*, 125, 439
Landau, L.D., Lifshitz, E.M. 1962, "Quantum Mechanics" (London:Pergamon)
Langer, N., Henkel, C. 1995, *Space Sci. Rev.* 74, 343
Larson, R.B. 1998, *MNRAS*, 301, 569
Limongi, M., Chieffi, A., 2003, *ApJ*, submitted
Maeder, A. 1992, *A&A*, 264, 105
Maciel, W., DaCosta, R.D.D., Uchida, M.M.M. 2003, *A&A*397, 667
Matteucci, F. 2001, "The Chemical Evolution of the Galaxy", *ASSL*, Kluwer Academic Publishers
Matteucci, F. 1986, *ApJ*, 305, L81
Matteucci, F., Chiosi, C. 1983, *A&A*, 123, 121
Matteucci, F., François, P. 1992, *A&A*, 262, L1
Matteucci, F., François, P. 1989, *MNRAS*, 239, 885
Matteucci, F., Greggio, L. 1986, *A&A*154, 279
Matteucci, F., Pipino, A. 2002, *ApJ*, 569, L69
Matteucci, F., Recchi, S., 2001, *ApJ*, 558, 351
Mannucci, F., Maiolino, R. et al. 2003, *astro-ph/0302323*
Marigo, P., Bressan, A., Chiosi, C. 1996 *A&A*, 313, 545
McWilliam, A., Rich, R.M. 1994, *ApJS*, 91, 7
Melendez, J., Barbuy, B. 2002, *ApJ*, 575, 474
Meynet, G., Maeder, A. 2002, *A&A*, 390, 561
Nakamura, J., Umeda, H. et al. 1999, *ApJ*, 193, 208
Nomoto, K., Iwamoto, N. et al. 1997, *Nuclear Physics*, A621, 467
Oey, M.S. 2000, *ApJ*, 542, L25
Pardi, M.C., Ferrini, F., Matteucci, F. 1995, *ApJ*, 444, 207
Pettini, M., Rix, S.R., Steidel, C.C. et al. 2002, *ApJ*, 569, 742
Portinari, L., Chiosi, C. 1999, *A&A*, 350, 827
Portinari, L., Chiosi, C., Bressan, A. 1998, *A&A*, 334, 505
Prantzos, N. 2000, *astro-ph/0210094*
Rauscher, T., Hoffman, R.D., Woosley, S.E. 2002, *ApJ*, 576, 323
Salpeter, E.E. 1955, *A&A*, 121, 161
Samland, M., Hensler, G., Theis, C. 1997, *ApJ*476, 544
Scalo, J.M. 1986 *Fund. Cosmic Phys.*, 11, 1
Scalo, J.M. 1998 in "The Stellar Initial Mass Function", *A.S.P. Conf. Ser.* Vol. 142 p.201
Schmidt, M. 1959, *ApJ*, 129, 243
Siess, L, Livio, M., Lattanzio, J. 2002, *ApJ*, 570, 329
Sommer-Larsen, J., Gotz, M, Portinari, L. 2002, *Astrophys. Space Science*, 281, 519
Talbot, R.J., Arnett, D.W. 1971, *ApJ*, 170, 409
Thielemann, F.K., Nomoto, K., Hashimoto, M. 1996, *ApJ*, 460, 408
Tinsley, B.M. 1979, *ApJ*, 229, 1046
Tinsley, B.M. 1980, *Fund. Cosmic Phys.*, 5, 287
Thomas, D., Greggio, L., Bender, R. 1998, *A&A*, 296, 119
Tornambé, A., Matteucci, F. 1986, *MNRAS*, 223, 69
Tosi, M. 1988 *A&A*197, 33
Tosi, M. 2000, in "The Chemical Evolution of the Milky Way: Stars versus Clusters", ed. F. Matteucci & F. Giovannelli, *Kluwer Academic Publ.*, p. 505
Tsujimoto, T., Shigeyama, T., Yoshii, Y. 1999, *ApJ*, 519, L63
Umeda, H., Nomoto, K. 2002, *ApJ*, 565, 385

F. Matteucci

- van den Hoek, L.B., Groenewegen, M.A.T. 1997 A&AS, 123, 305
Vladilo, G. 2002, A&A, 391, 407.
Ventura, P., D'Antona, F., Mazzitelli, I. 2002, A&A, 393, 21
Whelan, J., Iben, I. Jr. 1973, ApJ, 186, 1007
Woosley, S.E., Weaver, T.A. 1995, ApJS, 101, 181
Wyse, R.F.G., Silk, J. 1989, ApJ, 339, 700